View Article Online / Journal Homepage / Table of Contents for this issue

Published on 14 December 2005. Downloaded by National Taiwan University of Science and Technology on 6/23/2019 3:32:27 PM.

Dendritic nano- and microhydrogels fabricated by triethoxysilyl focal dendrons†

Daisuke Onoshima[a] and Toyoko Imae*[ab]

Received 28th October 2005, Accepted 6th December 2005
First published as an Advance Article on the web 14th December 2005
DOI: 10.1039/b515299b

Nano- and microhydrogels were fabricated in water by first to third generation triethoxysilyl focal poly(amido amine) dendrons with hexyl spacer. The focal points of dendrimers were hydrolyzed and covalent-bonded through the simple sol–gel process at an acidic or basic catalytic condition. The growth of aggregates and the following gel formation were determined by rapid increase and convergent steady value in light scattering of dendron solutions. The sol–gel reaction was also confirmed from the disappearance of an infrared absorption band of Si–O(C_2H_5) stretching vibration mode (1080 cm^{-1}) and the appearance of Si–O–Si stretching bands (1136 and 1049 cm^{-1}). The resultant gels were transparent and rather fluid. Transmission electron microscopic images of the gels showed three-dimensional dendritic growing of fine fibrils. The nanogel nuclei grew up favourably to nanogels in acidic conditions and to microgels in basic conditions, and the growth was more remarkable at higher generation of dendrimers. At high concentration of dendrimer, macrogels with fiber-like texture were formed. It was supported that siloxane-linked focal groups constructed main chains and branches of fibrils, and dendron side chains coated polysiloxane backbones. The hydrogels emitted fluorescence, which was stronger at base-catalyzed condition than at acid-catalyzed condition. This indicates that crowded circumstances or large amount of fluorescence-inducing moieties intensify the fluorescence. Fluorescent images of such architectures were visualized on a fluorescent microscope.

Introduction

Microgels, microscopic gel particles with intramolecularly cross-linked structure, are a unique type of Macromolecules Both their internal and surface properties can be controlled for a wide range of uses.[1] Since the first production by Bobalek *et al.*,[2] microgels have been applied to the coating, the sealing, and the thermoset materials by hybridizing with the resin, and relatively large particles over submicron size have been used as the column packing agents of the liquid chromatography and the reagent carriers in medical diagnostics.[3–6]

Microgels are mainly prepared by dispersion polymerization, emulsification polymerization, suspension polymerization and precipitation polymerization of multifunctional precursors in aqueous or non-aqueous medium. Then, surfactants are utilized to achieve the polymerization within isolated domains in submicron size.[3,7–10] The process towards microgelation constrains the size of the dispersed domains.

Recent advances in supramolecular assembly of dendrimers and dendrons provide a unique methodology to create dendritic architectures, which have attracted great attention as a new type of gelator.[11–14] Kim *et al.*[15] have reported comprehensive results on the formation of thermoreversible supramolecular gels through self-organization of some amide dendrons in organic media. The dendritic organo gelator based on dendrimers with benzyloxy-type peptide core has been reported by Jang *et al.*[16] Dvornic *et al.*[17] prepared a covalently cross-linked three-dimensional network from a sol–gel type hydrolysis of alkoxysilylterminated dendrimers, followed by a silanol condensation reaction. These gels may be viewed as covalently or noncovalently linked architectures constructed by dendrimer building blocks.

In the present work, the formation of uniquely structured nano- and microhydrogels consisting of functional dendrons with triethoxysilyl focal point has been investigated in an aqueous medium. The gelation reaction was promoted by two types of catalysts (acidic and basic). It was previously reported that the sol–gel process by hydrolysis reaction largely depends on the catalyst.[18–24] Using the simple sol–gel process, the focal points were connected by covalent bond in order to form nano- or microscopic aggregates (nanogels or microgels). The hydrogels were characterized by using scattering, spectroscopy and microscopy. The influence of gelation condition and dendron generation to the hydrogel formation was examined.

Experimental

First to third generation (G1–3) triethoxysilyl focal poly(amido amine) dendrons with hexyl spacer (Fig. 1) were synthesized *via* Michael addition of 3-aminopropyltriethoxysilane followed by amidation according to the previously reported method.[25] On a Michael addition reaction,

[a]*Graduate School of Science, Nagoya University, Chikusa, Nagoya 464-8602, Japan*
[b]*Research Center for Materials Science, Nagoya University, Chikusa, Nagoya 464-8602, Japan. E-mail: imae@nano.chem.nagoya-u.ac.jp; Fax: +81 52 789 5912; Tel: +81 52 789 5911*

† Electronic supplementary information (ESI) available: Time dependence of scattering intensity during gelation, UV–vis absorption spectra and generation dependence of emission intensity of dendron hydrogels. See DOI: 10.1039/b515299b

View Article Online

Published on 14 December 2005. Downloaded by National Taiwan University of Science and Technology on 6/23/2019 3:32:27 PM.

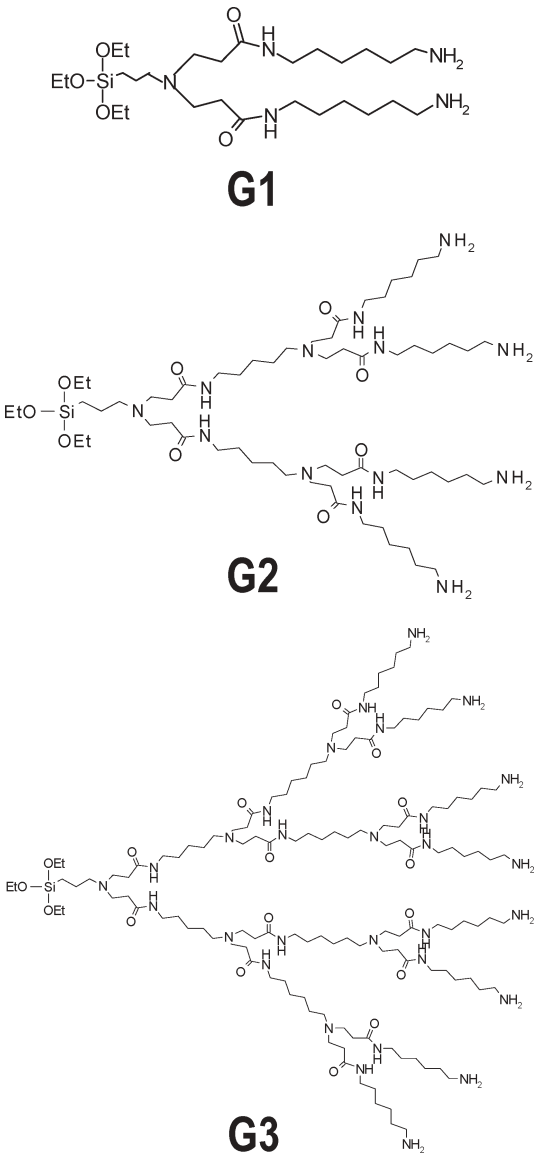

Fig. 1 Chemical structures of G1–3 triethoxysilyl focal dendrons.

methylacrylate in methanol was added dropwise in a methanol solution of 3-aminopropyltriethoxysilane or triethoxysilyl focal poly(amido amine) dendrons with amine terminals, and nitrogen gas was flushed. A Michael addition product was dissolved in methanol, and hexamethylene diamine in methanol was added dropwise under nitrogen atmosphere. Both reaction solutions were stirred at room temperature for 12 h, and excess solvent and unreacted reactants were removed by vacuum distillation. Methanol, hydrochloric acid and sodium hydroxide were purchased from Wako Pure Chemical Industries. Ltd. and were used without further purification. Water was purified by distillation and deionization using a Millipore Milli-Q Lab purification system and was used throughout all experiments.

The hydrolysis and polycondensation of triethoxysilyl focal dendrons were performed in aqueous solutions of hydrochloric acid or sodium hydroxide. The reaction solutions were stirred until it became clear (for $\sim$5 min) and allowed to stand at room temperature ($\sim$25 °C). A concentration of triethoxysilyl focal dendrons was 5 mg cm^{-3} except the examination of concentration dependence.

Dynamic light scattering (DLS) measurements were performed on an Otsuka Electronics DLS-700 (equipped with a 10 mW Ar ion laser, wavelength = 488 nm). Measurements were carried out at room temperature and at scattering angle of 45°. DLS data were analyzed using a CONTIN method on an ALV-5000/E Multiple Tau Digital Correlator. The hydrodynamic radius (R_h) of hydrogels was calculated using a Stokes–Einstein equation $R_h = k_B T/6\pi\eta D$, where k_B is the Boltzmann constant, T is the absolute temperature, η is the solvent viscosity, and D is the observed diffusion coefficient.

Infrared (IR) absorption spectra in the region of 4000–1000 cm^{-1} were recorded at room temperature on a Bio-Rad FTS 575C FT-IR spectrometer. Specimens were prepared by spreading a small drop of solutions onto CaF_2 windows and evaporating the solvent. Fluorescence spectra were recorded under excitation at different wavelengths on a Hitachi F-4010 fluorometer, and ultra violet (UV)–visible absorption spectroscopic measurements were performed on a Shimadzu UV-2200 instrument using a quartz cell (10 mm path).

Transmission and scanning electron micrographs (TEM, SEM) were taken on Hitachi H-7000 and JEOL JSM-6330F microscopes, respectively (operating at 100 and 15 kV, respectively). A drop of solution was placed onto a carbon-coated copper grid and air-dried. Atomic force micrographs (AFM) were taken on a Digital Instruments NanoscopeIII. Spin coating treatment (1600 rpm, 1 min) of a drop of solution was carried out on a mica substrate. A Nicon 80i fluorescent microscope with a filter DAPI was used to take images of nanogels. Air-drying of a drop of solution was carried out on a glass plate.

Results and discussion

Gelation process

Fig. 2 shows the time dependence of scattering intensity and hydrodynamic radius (R_h) on the gelation process of G3 triethoxysilyl focal dendrons in water (5 mg cm^{-3}). Both parameters increased rapidly and became constant. These

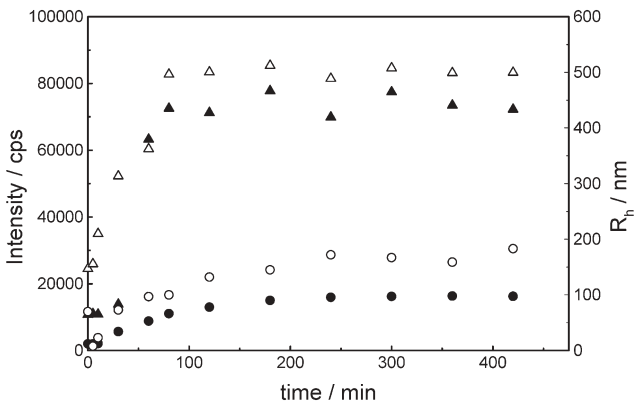

Fig. 2 Time dependence of scattering intensity (●: acid-catalyzed, ▲: base-catalyzed) and R_h (○: acid-catalyzed, △: base-catalyzed) during gelation of G3 dendron. Time "zero" indicates just after stirring.

 This journal is © The Royal Society of Chemistry 2006

View Article Online

Published on 14 December 2005. Downloaded by National Taiwan University of Science and Technology on 6/23/2019 3:32:27 PM.

behaviors imply the growth of aggregates, that is, the gelation and its completion.

In case of acidic condition, these values became constant after ~300 min, which was necessary for the completion of gelation. On the other hand, it was only about 100 min in basic conditions. It is common that the sol–gel reaction requires longer time in acidic conditions than in basic conditions.[18,20] Moreover, It took 90 to 120 min for the synthesis of siloxane wires or rods using sol–gel reaction.[26,27] However, half a day or overnight standing was required to get cross-linked polysiloxanes such as gel film.[28] Therefore, the gel formation in this report is close to the former case. In addition, the gelation was accomplished at shorter time for larger generation of dendron (see Fig. S1 in the electronic supplementary information (ESI)†).

Hydrolysis of dendrons

The change of the chemical structure of G3 triethoxysilyl focal dendron on the sol–gel process was examined by IR absorption spectra. As seen in Fig. 3, the IR spectrum of G3 dendron exhibited amide vibration bands of amide A and B at 3289 and 3081 cm^{-1}, respectively, amide I at 1643 cm^{-1}, amide II at 1555 cm^{-1} and amide III at 1369 cm^{-1}. In addition, there were additional bands of CH_2 antisymmetric and symmetric stretching modes at 2930 and 2853 cm^{-1} and a CH_2 bending mode at 1462 cm^{-1}.[24,29] These characteristic bands of the dendritic moiety were clearly seen in the spectra of both acid-catalyzed and base-catalyzed hydrogels. It was confirmed from the similarity in the features of three spectra in Fig. 3 that the chemical structure of the dendritic moiety of triethoxysilyl focal dendron was not changed during gelation.

After the sol–gel reaction, a Si–O stretching vibration band of $Si–OC_2H_5$ at 1080 cm^{-1} in a G3 dendron spectrum decreased, but Si–O–Si stretching bands appeared at 1136 and 1049 cm^{-1}. The spectrum of acid-catalyzed gel displayed both $Si–OC_2H_5$ and Si–O–Si stretching bands. This indicates imperfect sol–gel reaction of the focal point. On the other hand, only Si–O–Si bands existed in the spectrum of base-catalyzed gel. These results indicate that the focal point of G3 dendron was hydrolyzed, during the gelation process, more abundantly in basic conditions than in acidic conditions, in line with the light scattering results. A similar IR band variation has been reported on the process of siloxane linkage formation such as a sol–gel type hydrolysis of alkoxysilyl-terminated dendrimers in methanol and supramolecular organosilanes in ethyl acetate.[17,28]

The acid-catalyzed gel did not exhibit a NH_2 stretching band at 3395 cm^{-1}, but the base-catalyzed one did. The terminal amine group of triethoxysilyl focal dendon should be protonated in acidic conditions, as estimated from a pK_a (= 9.20) of terminal amine.[30] In addition, the dendron generation scarcely affected the IR spectra of gels.

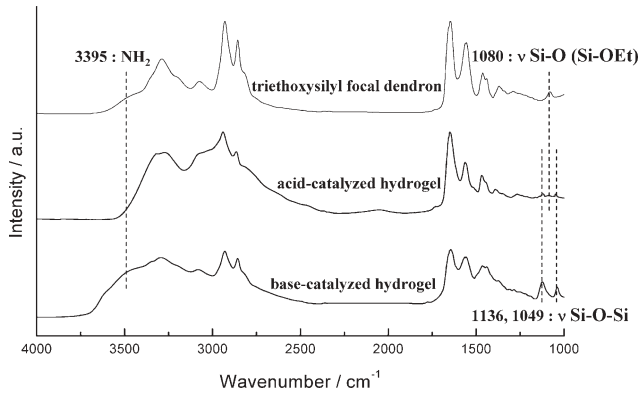

Fig. 3 IR absorption spectra of G3 dendron and hydrogels.

Morphology of gels

TEM images of triethoxysilyl focal dendron gels are shown in Fig. 4. In case of acid-catalyzed condition, gels at the submicron or less size (<500 nm) were well dispersed, indicating the formation of a "nanogel". As the generation of the dendrons increased, the size of the gels became large. It is supposed that these nanogels are composed of triethoxysilyl focal dendrons, which are connected by the siloxane linkages. On the other hand, dendritic textures (2–7 μm size) consisting of fine fibrils were observed in base-catalyzed conditions. These fibrils were bundled to become thicker fibers. These dendritic microgels grew up and the constituent fibers were crowded, as the generation of dendrons increases.

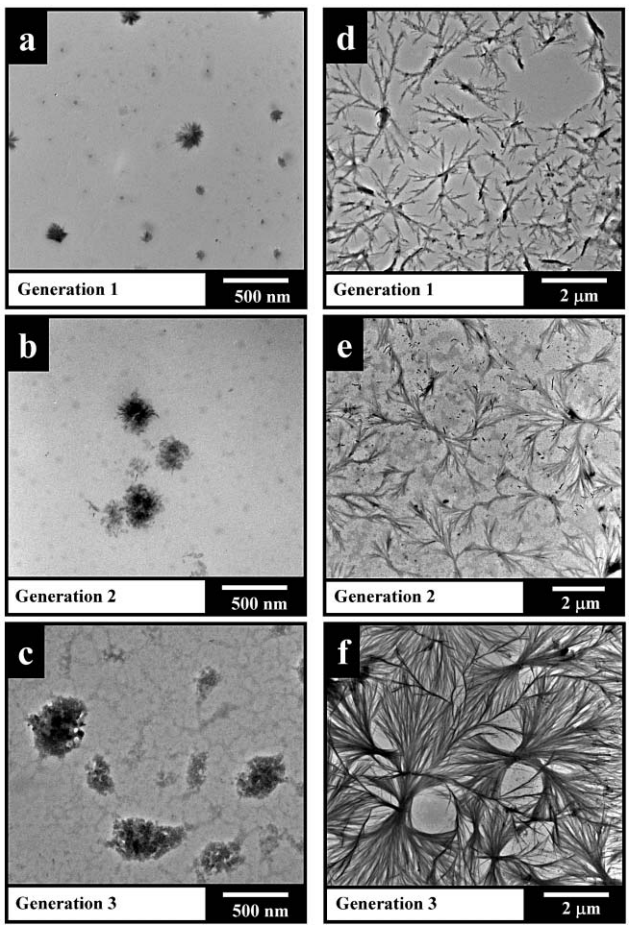

Fig. 4 TEM images of G1–3 dendron hydrogels. a, b, c: acid-catalyzed, d, e, f: base-catalyzed.

View Article Online

Published on 14 December 2005. Downloaded by National Taiwan University of Science and Technology on 6/23/2019 3:32:27 PM.

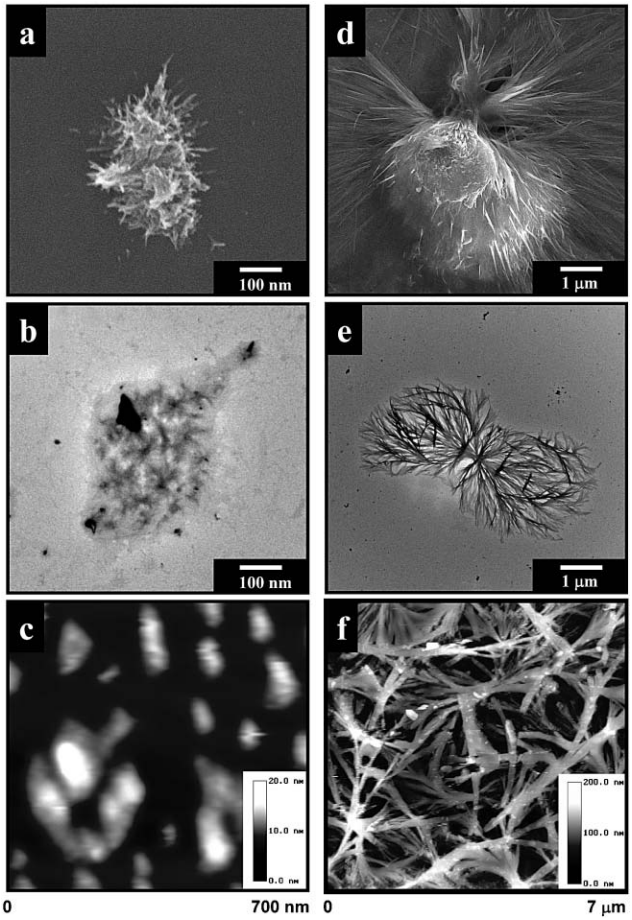

Fig. 5 Microscopic images (a, d: SEM, b, e: TEM, c, f: AFM) of G3 dendron hydrogels. a, b, c: acid-catalyzed, d, e, f: base-catalyzed.

Fig. 5 shows three types of microscopic observation of G3 dendron hydrogels. In the case of acid-catalyzed nanogels, the SEM image in Fig. 5a displayed the texture of a gel, which consists of a number of sharp-pointed needles. In the TEM image in Fig. 5b, the dendritic inner structure of the gel was clarified. These results indicate that the constituent element of the nanogel is the same as that of dendritic microgel formed in basic conditions. While the diameters of these gels were in the range of 300–500 nm, the height of gel estimated from AFM images in Fig. 5c was only ~20 nm, indicating the flattening of flexible gels on the substrate.

In case of base-catalyzed G3 dendron microgel, a SEM image in Fig. 5d displayed the dendritic growth of fibrils, the dense needle-like fibers at the center of the growth, and the soft down-like fibril structure at the periphery. The size of the dendritic microgel was approximated 5 μm from the TEM image in Fig. 5e. An AFM image of condensed microgels in Fig. 5f also confirmed the fibrous structure and its three-dimensional growth.

The hydrodynamic diameter of gels determined by DLS (Fig. 2) was 390 nm for acid-catalyzed nanogels and 980 nm for base-catalyzed microgels. Then, electron microscopic size of microgels in basic conditions seems different from hydrodynamic size. However, the morphology of these gels should be changeable depending on the condition: Each microgel tends to be a shrunk globule in solution and flatten on solid substrate. Therefore, the electron microscopic size of microgels seems to be larger than hydrodynamic size.

Fibril structure

The schematic fibril structure of triethoxysilyl focal dendron gel involving polysiloxane chain is illustrated in Fig. 6a, where the wedge dendron moieties bonded at the focal point are arranged radially in cross-sectional area of a fibril so as to avoid the steric hindrance. Since the calculated molecular dimension of G3 dendron is ~4.9 nm in length (Fig. 6b), the cross-sectional diameter of each unit fibril is estimated to be ~9.0 nm or more. This size is consistent with the observed fibril diameter (9.4 nm) in a SEM image in Fig. 6c and other micrographs displayed above (*e.g.*, 12 nm, the finest fibril in a TEM image in Fig. 4). Considering the fact that micro-order hydrogel was enlarged from nanogel nuclei, it is supposed that the fibril structure originates from the formation of the siloxane bonding between focal points. The siloxane bonding grows as a main chain and a branch: Siloxane bonding happens not only at two but also at three functional triethoxysilane groups in a molecule, and, therefore, the branched fibril growth as shown in Fig. 6a occurs during the sol–gel reaction.

Here, amine terminal groups on dendron moiety may be hydrogen-bonded each other to form bundles. Though the

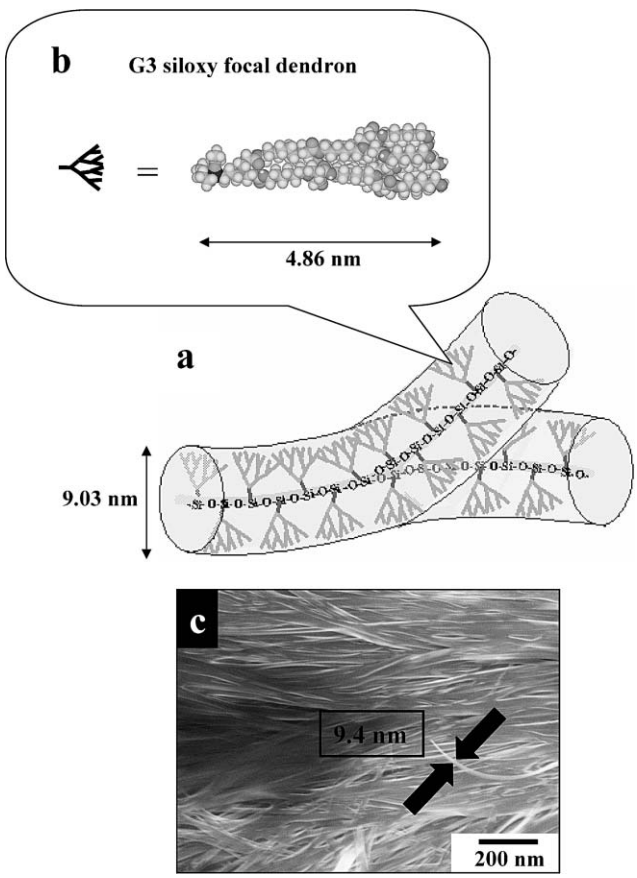

Fig. 6 Schematic illustration of fibril (a), molecular graphic of G3 dendron (b) and SEM image of microgels in basic conditions (c).

 This journal is © The Royal Society of Chemistry 2006

View Article Online

Published on 14 December 2005. Downloaded by National Taiwan University of Science and Technology on 6/23/2019 3:32:27 PM.

electrostatic repulsion between the positively charged terminal groups can occur, the bundle formation is often possible to be reinforced by the hydrophobic interaction between alkyl chains in the spacer. However, peripheral hydrophilic terminal groups located on the periphery of the gels may affect on the favorable dispersibility of the gels.

pH effect on gelation

The pH effect on two types of gels was tested by jumping the acidic and basic conditions. When sodium hydroxide was added to the transparent acid-catalyzed G3 dendron nanogel dispersion (Fig. 7a), the mixture turned to a turbid dispersion (Fig. 7b) and finally became transparent again (Fig. 7c), indicating that the sol–gel reaction of the residual unreacted precursors proceeded. The change of TEM image from Fig. 7d to Fig. 7e clearly reveals the needle-like growth from nanogels. This type of growth is similar to the growth of microgels at intrinsically base-catalyzed condition. Obviously, these results are consistent with the IR result in Fig. 3, which indicates that the sol–gel reaction at focal points of dendrons was not completed under the acidic condition. Furthermore, since the amine terminal groups of triethoxysilyl focal dendron is deprotonated at the basic condition, the hydrogen-bonding association of dendron moieties is facilitated.

On the other hand, even if hydrochloric acid was added to the base-catalyzed G3 dendron gels, there was no noticeable difference in microgels, as seen in TEM results before and after adding acid into the base-catalyzed gels (Fig. 8). Therefore, it can be assumed that the base-catalyzed microgels are already

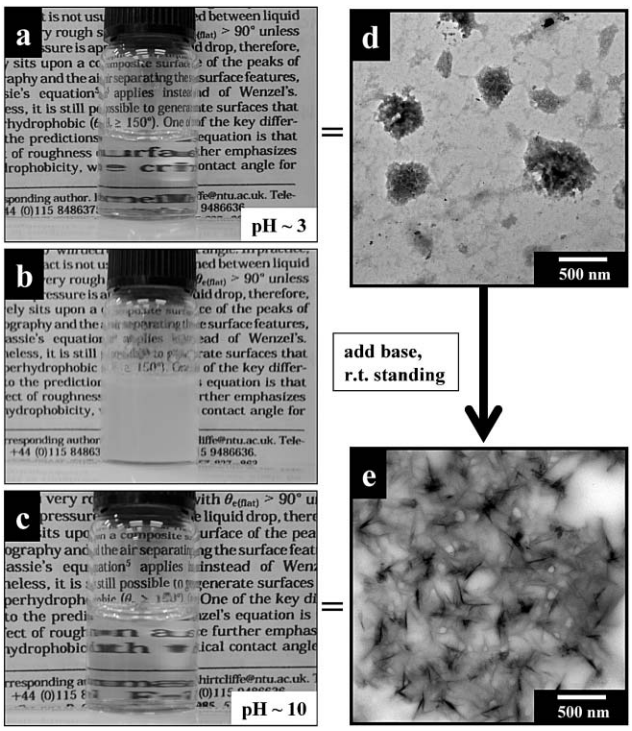

Fig. 7 pH jump of acid-catalyzed G3 dendron nanogels. a: acid-catalyzed microgels, b: just after adding sodium hydroxide, c: after standing overnight at room temperature, d: TEM image of (a), e: TEM image of (c).

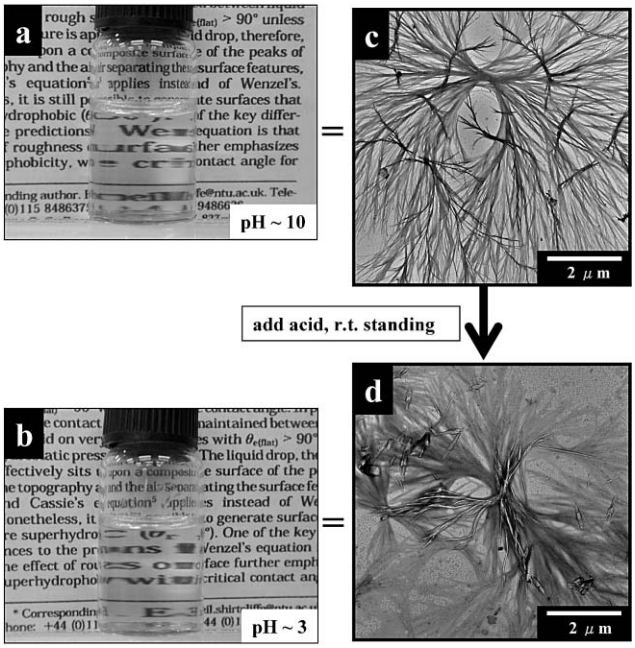

Fig. 8 pH jump of base-catalyzed G3 dendron microgels. a: base-catalyzed microgels, b: after adding hydrochloric acid and standing overnight at room temperature, c: TEM image of (a), d: TEM image of (b).

completed, as estimated from an IR absorption spectrum, too (Fig. 3), and the structure consisting of siloxane bonding is unchangeable at strong acid.

Concentration dependence of gelation

The gel formation of G3 triethoxysilyl focal dendron at acid- and base-catalyzed conditions was investigated at different dendron concentrations. The dendrons at 0.05–20 mg cm^{-3} in water formed tansparent dispersions (see the bottles in Fig. 7 and 8), which contain the nano- or microgels. On the other hand, when a 50 mg cm^{-3} solution of dendron was stirred and allowed to stand at room temperature, it gradually became viscous and finally turned non-flowing translucent gels. Then, the transition concentration (20–50 mg cm^{-3}) to non-fluid gels is comparable to those of other gels based on dendrimers or dendrons.[15,16] The formation of the non-fluid gels was thermo-reversible in aqueous media: These gels were dissolved to be fluid at ~60 °C. After cooling to room temperature, non-fluid gels were recovered with passing time, supporting the formation of noncovalent-bonded network.

TEM images of the non-fluid gels of G3 triethoxysilyl focal dendron prepared with acidic and basic catalysts displayed network structures, as seen in Fig. 9. Macrogels in acidic conditions consisted of network of nanogels: Particles (nanogels) interacted with each other to form network. Meanwhile, macrogels in basic conditions exhibited the morphology of thin fibrils and their bundles. While the report of the former type of networks is less, the latter has been reported by many workers.[31] Thin fibrils should be a polysiloxanes with dendron side chains, and they interact each other to form bundles.

These results indicate that the dendrons at high concentration in aqueous media form networks of polysiloxane

View Article Online

Published on 14 December 2005. Downloaded by National Taiwan University of Science and Technology on 6/23/2019 3:32:27 PM.

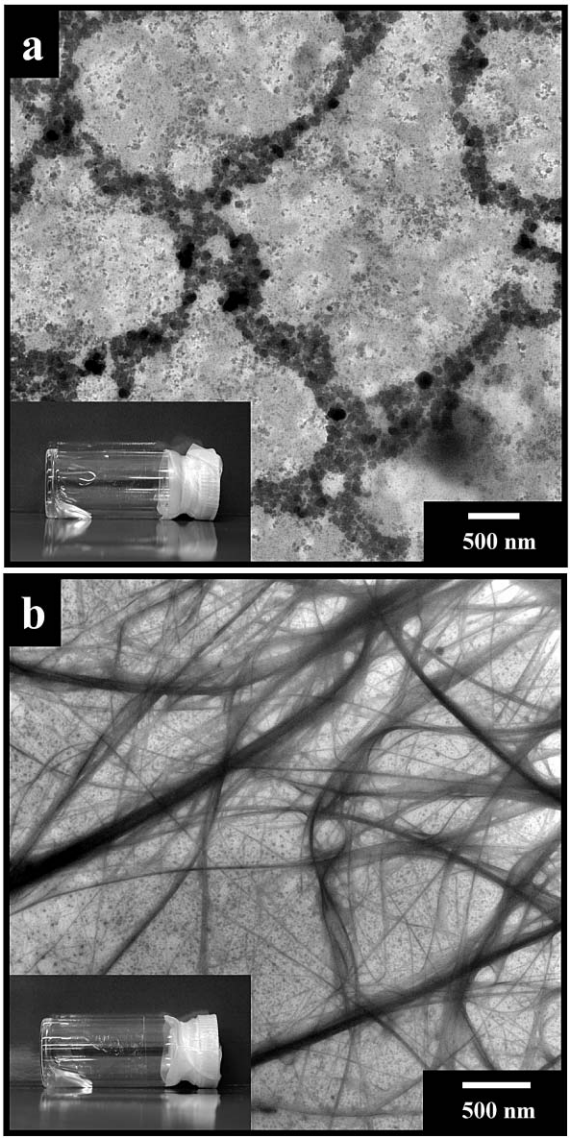

Fig. 9 TEM images of G3 dendron macrogels (concentration: 50 wt%). The insets are photos of non-fluid hydrogels. a: acid-catalyzed, b: base-catalyzed.

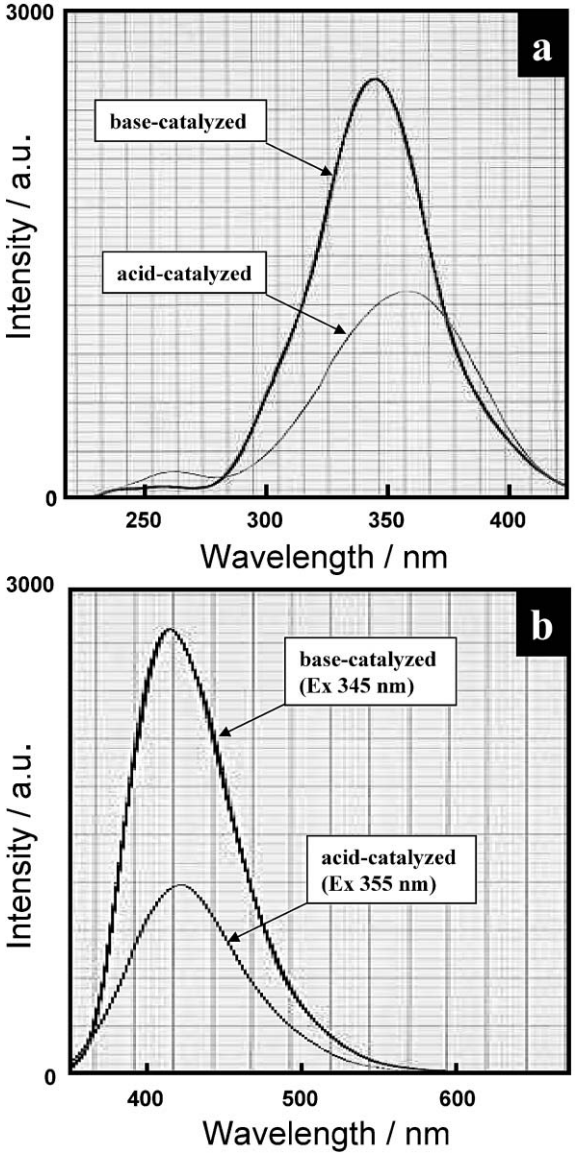

Fig. 10 Fluorescence spectra of G3 dendron hydrogels. a: Excitation spectra emitted at 428 nm. b: Emission spectra excited at different wavelengths.

architectures (particles or fibers). Architecture in acidic conditions bears comparison, in size and shape, with that of nanogels in dilute conditions. On the other hand, fibrils in basic conditions resulted from the one-dimensional polymerization of triethoxysilyl groups without branching reaction. Then, the network structure is due to the non-covalent bonding of polysilane architectures such as van der Waals and hydrogen bonding interactions, and therefore, structural breakdown and re-formation can occur depending on temperature.

Luminescence properties of gels

Fig. 10 shows excitation and emission fluorescence spectra of G3 triethoxysilyl focal dendron hydrogels at dilute concentrations. Acid-catalyzed nanogels present an excitation band at 355 nm and an emission band at 428 nm. In comparison with acid-catalyzed nanogels, base-catalyzed microgels produced similar fluorescence bands but showed strong intensity. UV–Visible absorption spectra of these hydrogels indicated that there were no remarkable UV–visible absorption bands around the fluorescence excitation bands (see Fig. S2 in the ESI†). Meanwhile, the emission intensity of triethoxysilyl focal dendron hydrogels increased with the generation (see Fig. S3 in the ESI†), while the emission band position scarcely changed.

Importantly, luminescence phenomena from poly(amido amine) dendrimers and dendrons have been reported.[32–36] Wang and Imae[34] found pH-dependent fluorescence property of poly(amido amine) dendrimers and they explained that the dendrimer structure or the microenvironment of the functional groups, such as tertiary amine groups along dendritic branches, played a key role in inducing the fluorescence. In the present study, the fluorescence was stronger in basic

 This journal is © The Royal Society of Chemistry 2006

View Article Online

Published on 14 December 2005. Downloaded by National Taiwan University of Science and Technology on 6/23/2019 3:32:27 PM.

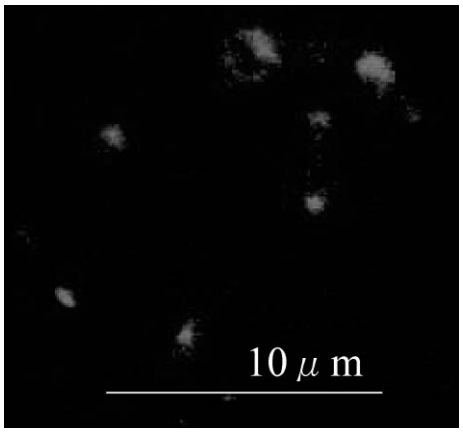

Fig. 11 A fluorescence microscopic image of acid-catalyzed G3 dendron nanogels.

conditions and high generation than in acidic conditions and low generation, depending on the growth in morphological structure of hydrogels. This suggests that the difference in morphological structure or localized fluorescence-inducing moieties between acid-catalyzed nanogels and base-catalyzed microgels significantly influenced the fluorescence properties rather than the difference in dendritic chemical structure such as the number of functional amine groups and protonation.

Fig. 11 displays a fluorescence microscopic image of nanogels prepared in acidic conditions. Fluorescent spots are visualized, and their sizes were almost equal to those from TEM.

Conclusions

Nano- and microstructured polysiloxane materials have been synthesized by sol–gel reaction of triethoxysilyl focal dendrons, which was catalyzed by hydrochloric acid and sodium hydroxide. Polysiloxane fibrils fabricated by dendrons grew up to be hydrogels with dendritic morphology, although the sizes of gels depended on dendrimer generation and catalyst (acidic or basic). This is the first investigation of the preparation of size-controllable hydrogels consisting of siloxane bonds and dendron side chains. The advantage of the present work is the potentials on the construction of water-soluble silica materials, of hybrid polymer materials with organic and inorganic components, or of core–shell polymer materials with branched backbone and dendronized shell. It should be also noticed from a viewpoint of the utilization as a fluorescent marker, because hydrogels emit fluorescence and detected as fluorophors on a fluorescence microscope. This is the first report where the fluorescence of poly(amido amine) dendrimer architecture was visualized by a microscope.

Acknowledgements

We gratefully thank Nicon Co. for the use of a fluorescence microscope and the helpful discussion. The present work was partly supported by the Grant-in-Aid for Scientific Research (B) (15350067) and by the Grant-in-Aid for Scientific Research in Priority Area "Molecular Nano Dynamics" from Ministry of Education, Culture, Sports, Science and Technology (MEXT), Japan.

References

1 J. Zhang, S. Xu and E. Kumacheva, *J. Am. Chem. Soc.*, 2004, **126**, 7908.
2 E. G. Bobalek, E. R. Moore, S. S. Levy and C. C. Lee, *J. Appl. Polym. Sci.*, 1964, **8**, 625.
3 (*a*) G. H. Ma and T. Fukutomi, *J. Appl. Polym. Sci.*, 1991, **43**, 1451; (*b*) G. H. Ma, T. Fukutomi and S. Nozaki, *J. Appl. Polym. Sci.*, 1993, **47**, 1243.
4 K. Ogawa, B. Wang and E. Kokufuta, *Langmuir*, 2001, **17**, 4704.
5 N. Murthy, Y. X. Thng, S. Schuck, M. C. Xu and J. M. J. Fréchet, *J. Am. Chem. Soc.*, 2002, **124**, 12398.
6 I. Gorelikov, L. M. Field and E. Kumacheva, *J. Am. Chem. Soc.*, 2004, **126**, 15938.
7 (*a*) X. Lu, Z. Hu and J. Gao, *Macromolecules*, 2000, **33**, 8698; (*b*) X. Xia, S. Tang, X. Lu and Z. Hu, *Macromolecules*, 2003, **36**, 3695.
8 S. Peng and C. Wu, *Macromolecules*, 2001, **34**, 568.
9 J. I. Amalvy, E. J. Wanless, Y. Li, V. Michailidou and S. P. Armes, *Langmuir*, 2004, **20**, 8992.
10 T. Hoare and R. Pelton, *Macromolecules*, 2004, **37**, 2544.
11 (*a*) V. Percec, W.-D. Cho, M. Möller, S. A. Prokhorova, G. Ungar and D. J. P. Yeardley, *J. Am. Chem. Soc.*, 2000, **122**, 4249; (*b*) V. Percec, W. D. Cho and G. Ungar, *J. Am. Chem. Soc.*, 2000, **122**, 10273; (*c*) V. Percec, W. D. Cho, G. Ungar and D. J. P. Yeardley, *J. Am. Chem. Soc.*, 2001, **123**, 1302.
12 (*a*) C. Marmillon, F. Gauffre, T. Gulik-Krzywicki, C. Loup, A.-M. Caminade, J.-P. Majoral, J.-P. Vors and E. Rump, *Angew. Chem., Int. Ed.*, 2001, **40**, 2626; (*b*) A. E. Ghzaoui, F. Gauffre, A.-M. Caminade, J.-P. Majoral and H. Lannibois-Drean, *Langmuir*, 2004, **20**, 9348.
13 (*a*) E. R. Zubarev, M. U. Pralle, E. D. Sone and S. I. Stupp, *J. Am. Chem. Soc.*, 2001, **123**, 4105; (*b*) E. R. Zubarev, M. U. Pralle, E. D. Sone and S. I. Stupp, *Adv. Mater.*, 2002, **14**, 198.
14 (*a*) C. S. Love, A. R. Hirst, V. Chechik, D. K. Smith, I. Ashworth and C. Brennan, *Langmuir*, 2004, **20**, 6580; (*b*) A. R. Hirst and D. K. Smith, *Langmuir*, 2004, **20**, 10851.
15 (*a*) C. Kim, K. T. Kim, Y. Chang, H. H. Song, T.-Y. Cho and H.-J. Jeon, *J. Am. Chem. Soc.*, 2001, **123**, 5586; (*b*) C. Kim, S. J. Lee, I. H. Lee and K. T. Kim, *Chem. Mater.*, 2003, **15**, 3638; (*c*) H. S. Ko, C. Park, S. M. Lee, H. H. Song and C. Kim, *Chem. Mater.*, 2004, **16**, 3872.
16 (*a*) W.-D. Jang, D.-L. Jiang and T. Aida, *J. Am. Chem. Soc.*, 2000, **122**, 3232; (*b*) W.-D. Jang and T. Aida, *Macromolecules*, 2003, **36**, 8561.
17 P. R. Dvornic, J. Li, A. M. de Leuze-Jallouli, S. D. Reeves and M. J. Owen, *Macromolecules*, 2002, **35**, 9323.
18 A. H. Boonstra and J. M. E. Baken, *J. Non-Cryst. Solids*, 1990, **122**, 171.
19 Y. Chujo, S. Kure, H. Matsuki and T. Saegusa, *Proc. Jpn. Acad.*, 1994, **70**, 138.
20 K. G. Sharp, *J. Sol-Gel Sci. Technol.* , 1994, **2**, 35.
21 T. N. M. Bernards, M. J. C. H. Janssen and M. J. van Bommel, *J. Non-Cryst. Solids*, 1994, **168**, 201.
22 (*a*) Y. Kaneko, N. Iyi, T. Matsumoto, K. Fujii, K. Kurashima and T. Fujita, *J. Mater. Chem.*, 2003, **13**, 2058; (*b*) Y. Kaneko, N. Iyi, K. Kurashima, T. Matsumoto, T. Fujita and K. Kitamura, *Chem. Mater.*, 2004, **16**, 3417.
23 S. H. Kim, B. Y. H. Liu and M. R. Zachariah, *Langmuir*, 2004, **20**, 2523.
24 G. Kwak, A. Takagi, T. Fujiki and M. Masuda, *Chem. Mater.*, 2004, **16**, 781.
25 Y. Omprakash, M. Ujihara and T. Imae, *Trans. Mater. Res. Soc. Jpn.*, 2004, **29**, 165.
26 L. M. Bronstein, C. Linton, R. Karlinsey, B. Stein, D. I. Svergun, J. W. Zwanziger and R. J. Spontak, *Nano Lett.*, 2002, **2**, 873.
27 B. L. V. Prasad, S. I. Stoeva, C. M. Sorensen, V. Z. Zaikovski and K. J. Klabunde, *J. Am. Chem. Soc.*, 2003, **125**, 10488.
28 J. T. Han, D. H. Lee, C. Y. Ryu and K. Cho, *J. Am. Chem. Soc.*, 2004, **126**, 4796.
29 (*a*) A. Manna, T. Imae, K. Aoi, M. Okada and T. Yogo, *Chem. Mater.*, 2001, **13**, 1674; (*b*) M. Ito, T. Imae, K. Aoi,

View Article Online

Published on 14 December 2005. Downloaded by National Taiwan University of Science and Technology on 6/23/2019 3:32:27 PM.

K. Tsutsumiuchi, H. Noda and M. Okada, *Langmuir*, 2002, **18**, 9757.
30 D. Leisner and T. Imae, *J. Phys. Chem. B*, 2003, **107**, 13167.
31 (*a*) T. Tachiban and H. Kambara, *J. Am. Chem. Soc.*, 1965, **87**, 3015; (*b*) N. Nakashima, S. Asakuma and K. Kunitake, *J. Am. Chem. Soc.*, 1986, **107**, 509; (*c*) R. H. Wade, P. Terech, E. A. Hewat, R. Ramasseul and F. Volino, *J. Colloid Interface Sci.*, 1986, **114**, 442; (*d*) J.-H. Fuhrhop, P. Schnieder, J. Rosenberg and E. Boekema, *J. Am. Chem. Soc.*, 1987, **109**, 3387; (*e*) H. Yanagawa, Y. Ogawa, H. Furuta and K. Tsuno, *J. Am. Chem. Soc.*, 1989, **111**, 4567; (*f*) T. Imae, Y. Takahashi and H. Muramatsu, *J. Am. Chem. Soc.*, 1992, **114**, 3414; (*g*) T. Imae, N. Hayashi, T. Matsumoto, T. Tada and M. Furusaka, *J. Colloid Interface Sci.*, 2000, **225**, 285; (*h*) K. Hanabusa, K. Okui, K. Karaki, T. Koyama and H. Shirai, *J. Chem. Soc., Chem. Commun.*, 1992, 1371; (*i*) T. Gulik-Krzywicki, C. Fouquey and J.-M. Lehn, *Proc. Natl. Acad. Sci. U. S. A.* , 1993, **90**, 163; (*j*) S. Bonaccio, M. Wessicken, D. Berti, P. Walde and P. L. Luisi, *Langmuir*, 1996, **12**, 4976; (*k*) T. Shimizu, M. Kogiso and M. Masuda, *Nature*, 1996, **383**, 487; (*l*) T. Imae, M.-P. Krafft, F. Giulieri, T. Matsumoto and T. Tada, *Prog. Colloid Polym. Sci.*, 1997, **106**, 52; (*m*) T. Imae, L. Gagel, C. Tunich, G. Platz, T. Iwamoto and K. Funayama, *Langmuir*, 1998, **14**, 2197; (*n*) V. Emmanouil, M. El Ghoul, C. André-Barrès, B. Guidetti, I. Rico-Lattes and A. Lattes, *Langmuir*, 1998, **14**, 5389; (*o*) T. Imae, Y. Ikeda, M. Iida, N. Koine and S. Kaizaki, *Langmuir*, 1998, **14**, 5631; (*p*) N. Yamada, K. Ariga, M. Naito, K. Matsubara and E. Koyama, *J. Am. Chem. Soc.*, 1998, **120**, 12192.
32 J. Zheng, J. T. Petty and R. M. Dickson, *J. Am. Chem. Soc.*, 2003, **125**, 7780.
33 W. I. Lee, Y. Bae and A. J. Bard, *J. Am. Chem. Soc.*, 2004, **126**, 8358.
34 D. Wang and T. Imae, *J. Am. Chem. Soc.*, 2004, **126**, 13204.
35 D. Wang and T. Imae, *Chem. Lett.*, 2005, **34**, 640.
36 C. Hirano, T. Imae, M. Tamura and Y. Takaguchi, *Chem. Lett.*, 2005, **34**, 862.

Chemical Biology

An exciting news supplement providing a snapshot of the latest developments in chemical biology

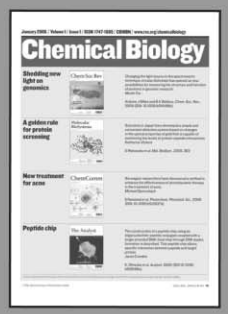

Free online and in print issues of selected RSC journals!*

Research Highlights – newsworthy articles and significant scientific advances

Essential Elements – latest developments from RSC publications

Free links to the full research paper from every online article during month of publication

*A separately issued print subscription is also available

30110553

RSC Publishing

www.rsc.org/chemicalbiology

 This journal is © The Royal Society of Chemistry 2006